Image Technology Investigation Based on Fingerprint Devices and Artificial Intelligence

Xuemei Zhao
School of Information Engineering, Yancheng Institute of Technology, Yancheng, 224000, China

***Abstract*—In response to the inaccurate visual positioning of fingerprint data images in investigative techniques, a new method based on wireless networks and artificial intelligence is proposed. The new method integrates wireless networks and image vision, while enhancing fingerprint data and images using cross temporal generative networks and channel state information. The research results indicated that the maximum positioning error value of the new model was 1.3m, which was 0.7m, 0.2m, and 0.4m lower than other models. The minimum positioning error value in indoor environments was 0.9m, which was lower compared with the 1.0m, 1.4m, and 1.6m of other models. The model used in the study had higher localization performance and recognition accuracy. The average accuracy was improved by about 4.5% compared with the TDF method with the lowest accuracy. The average root mean square error value was relatively low, with a minimum of 2.15. Compared with the highest SDF model, it was 4.43 lower. Therefore, the proposed method has better fingerprint recognition localization and investigation techniques, which has a better research guidance role for fingerprint localization and image recognition localization.**

***Keywords*—Investigation technology; fingerprint devices; image vision; fingerprint localization; image recognition**

I. Introduction

In the digital age, crime investigation technology is rapidly developing, especially in terms of fingerprint recognition accuracy and efficiency [1]. With the advancement of technology, traditional fingerprint recognition technology has been combined with new artificial intelligence technologies, making it more widely applied [2]. Fingerprint recognition technology is currently one of the most widely used identification methods. Its uniqueness and invariance make it an indispensable tool in criminal investigation [3]. However, with the increasing complexity and high technology of criminal methods, relying solely on traditional fingerprint recognition technology cannot meet the needs of modern investigation [4]. Therefore, artificial intelligence has been introduced into fingerprint recognition, especially in image processing and fingerprint localization analysis. It can not only greatly improve the speed and accuracy of recognition, but also identify and analyze complex fingerprint samples that are previously difficult to process. Therefore, the study combines wireless networks with fingerprint localization. Visual images are fused to expand the localization effect of current fingerprint data, and improve the accuracy of fingerprint localization. Secondly, Cross Temporal Generative Network (CTGN) and Channel State Information (CSI) are used to enhance fingerprint data to ensure that the current model can locate and investigate different environments and improve the effectiveness. The main purpose of the research is to explore how to improve the efficiency and accuracy of criminal investigation work by combining advanced fingerprint recognition equipment and artificial intelligence image technology. The study is divided into five sections. Section II reviews domestic and foreign research. Section III is about design research methods. Section IV analyzes the effectiveness of the model. Section V is a summary of the paper.

II. Related Works

In the current digital age, fingerprint recognition, as a highly reliable and accurate identity authentication technology, has been widely applied in the legal enforcement and personal security. Zhu et al. found that current fingerprint localization techniques became increasingly widespread, but there was still limited offline training for noise anti-interference. Therefore, a new indoor positioning method was proposed in the study using generalized learning systems. The new method could locate and analyze indoor fingerprint data through offline data training, while using principal component analysis to analyze data to reduce complexity. The research results indicated that the proposed method significantly shortened model training time and improved model accuracy [5]. Labinghisa et al. found that fingerprint authentication indoors required a significant amount of time. Meanwhile, there were more data issues with access points in the environment. Therefore, a new neural network fingerprint recognition method was proposed, which could improve the efficiency of model training and data collection. The research results indicated that the new method could improve the effectiveness and efficiency of indoor fingerprint localization [6]. The existing indoor positioning methods cannot effectively achieve high-precision positioning. Therefore, Zhang et al. proposed a beam antenna to enhance fingerprint localization method. The new method used beam antennas to locate fingerprint information, which was equipped with multiple antennas to improve positioning accuracy. The research results showed that the new method could accept fingerprint signals and improve the positioning effect of the model [7]. Traditional transfer learning algorithms have various problems and cannot effectively locate fingerprint information in space. Therefore, Li et al. proposed a new framework model for fingerprint localization. The new model could perform localization analysis on the spatial domain by removing redundant data information, improving the localization effect on fingerprint images. The research results indicated that the new method significantly enhanced the positioning accuracy of the model [8].

In indoor fingerprint localization, fingerprint integration can achieve better fingerprint information localization, but the limitations of improving fingerprint localization performance through this method are also obvious. Therefore, Zhou et al. proposed a fingerprint localization method based on deep learning. The new method mixed the received signals and fingerprint channel states to locate and analyze fingerprints. The research results indicated that the new method had better localization performance than traditional methods [9]. Li et al. proposed a new method based on Siamese convolutional neural network learning to achieve high-precision localization of fingerprint signal data. The new method improved the effectiveness of fingerprint localization by locating CSI within the same time interval. The research results indicated that the new method could effectively reduce fingerprint localization errors and improve localization performance compared with existing methods [10]. In the localization of fingerprint signals, frequency and geomagnetic signals can effectively locate fingerprints. Meanwhile, traditional signal acquisition may be affected by signal bias, resulting in labeling errors. Therefore, Tan et al. proposed a new method that combines frequency and geomagnetic signals. The new method could correlate spatial signals without artificial interference. The research results indicated that the new method could effectively improve the accuracy of fingerprint localization [11]. Li et al. found that most studies on fingerprint localization have been put on hold due to the large workload of offline data collection. Therefore, a new method based on Markov state iteration was proposed to address this issue, which utilized storage sources to solve the signal reception strength. The research results indicated that the new method could reduce the workload of offline data collection and improve positioning accuracy [12].

In summary, most of the current research on fingerprint localization and recognition mainly focuses on offline data collection and localization accuracy of fingerprint localization. Meanwhile, there are still some problems in current research, such as weak signal reception data, poor fingerprint positioning effect, and insufficient data processing accuracy. Therefore, a new model combining image technology and time-domain spatial algorithm is proposed. The new model accurately locates fingerprint data information through intelligent networks and CSI. Afterwards, time-domain spatial algorithms are used to integrate fingerprint images with data processing, thereby improving the accuracy and data processing performance of the model.

III. Design of Fingerprint Device and Artificial Intelligence Image Localization and Investigation Technology

This section mainly elaborates on the positioning methods of currently used fingerprint devices and the fusion technology of image vision. How to improve the accuracy of fingerprint localization and image recognition using current models has been analyzed, and data augmentation methods and localization models have been introduced.

A. Visual Efficient Image Investigation Fusion Technology

Wireless networks and biological vision signals have interoperability in locating location information. Integrating these two methods can achieve efficient localization of fingerprint devices. However, there are still many issues with the current methods used. CSI in wireless networks often fails to consider the relative position of the wireless network when performing data feature localization, resulting in inaccurate data information obtained [13]. Secondly, in the fusion of wireless networks and visual images, the position signal connection between the two is not sufficient, which leads to poor utilization of data information between the two. Finally, in the fused model, the two parts of data feature extraction and image fusion are independent of each other, making the processing process more complex and resulting in inaccurate positioning of fingerprint devices. Therefore, a new fingerprint device and image fusion model is designed, as shown in Fig. 1.

From Fig. 1, the model consists of three modules: location information collection module, data fusion module, and location detection module. The location information collection module mainly incorporates two data collection networks. Network channels collect feature data of the current visual image. A low orbit parameter fusion method is used in the data fusion module, which enables the model to maintain efficient vector fusion even with low computational complexity. The location detection module mainly classifies and predicts location information. The loss function is calculated to achieve end learning of the model. The network structure in the location information collection module is shown in Fig. 2.

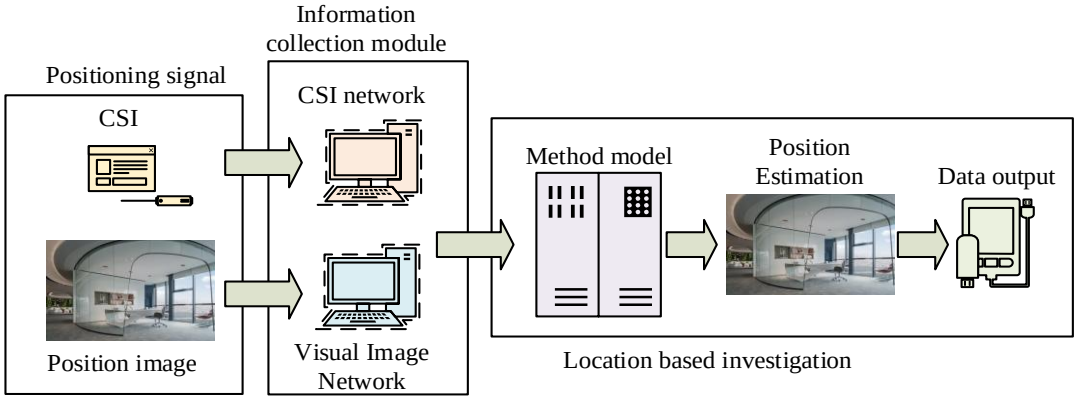

Fig. 1. Fingerprint device and image fusion model.

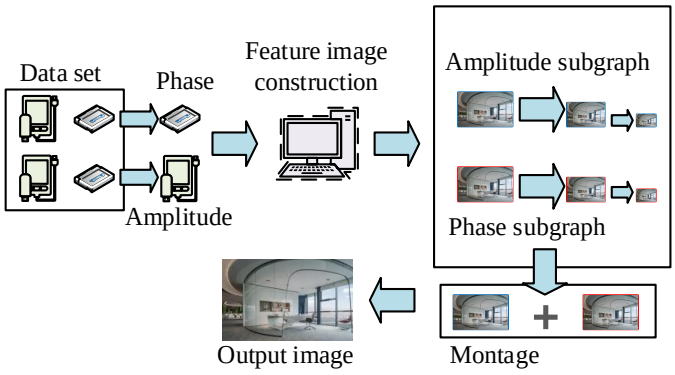

Fig. 2. Network structure of the location information collection module.

From Fig. 2, the CSI feature data image mainly collects position correction and amplitude of visual space images. Afterwards, the collected data is divided into amplitude sub-graphs and phase sub-graphs. The amplitude sub-graph expands and shrinks the image data, organizing it into a small data image. The same phase sub-graph also reduces or enlarges the features of the image data. The data features obtained from both are concatenated and fused to obtain usable data vector images. The process of building CSI involves collecting and using data. The carrier size of the wireless network is shown in Eq. (1) [14].

$$CSI_{m,n} = \left|CSI_{m,n}\right| \exp(j \angle CSI_{m,n}) \tag{1}$$

In Eq. (1), $\left|CSI_{m,n}\right|$ represents the amplitude value of the n-th wave in the m vectors. $\angle CSI_{m,n}$ represents the phase value of the n-th wave in m vectors. $1 \le m \le M, 1 \le n \le N$. Different wireless network lines are sorted by amplitude values to obtain the amplitude value matrix, as shown in Eq. (2).

$$AMP = \begin{bmatrix} \left|CSI_{1,1}\right| & \cdots & \left|CSI_{1,N}\right| \\ \vdots & \ddots & \vdots \\ \left|CSI_{M,1}\right| & \cdots & \left|CSI_{M,N}\right| \end{bmatrix} \tag{2}$$

In Eq. (2), AMP represents the amplitude matrix. The initial data collected may experience offset and delay. Therefore, the position information is corrected. Eq. (3) shows the size of the phase correction matrix [15].

$$PHA = \begin{bmatrix} \angle CSI_{1,1} & \cdots & \angle CSI_{1,N} \\ \vdots & \ddots & \vdots \\ \angle CSI_{M,1} & \cdots & \angle CSI_{M,N} \end{bmatrix} \tag{3}$$

In Eq. (3), PHA represents the size of the phase matrix. Through matrix size data analysis, the obtained matrices are fused to obtain the network input data. Meanwhile, to make feature data extraction more unified in the model, a new feature data extraction network is built based on network shared data, as shown in Fig. 3.

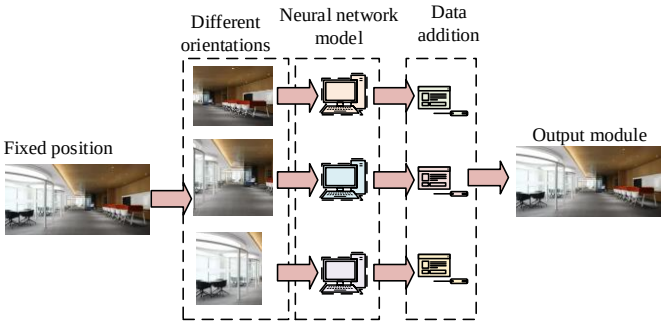

Fig. 3. Feature data extraction network.

From Fig. 3, after obtaining image data of a scene, visual information from different orientations of the image is first collected. Secondly, the collected image data is input into a convolutional neural network, where each convolutional layer can share the same network data. The images are added according to their positions to output feature data. The orientation information of the image is difficult to determine. Therefore, when extracting feature data, the direction information of the current data needs to be determined. Eq. (4) shows the image structure processed by the convolutional network [16].

$$h_{IMA}^{i} = shared_{CNN(image_i)} \tag{4}$$

In Eq. (4), $shared_{CNN}$ represents the shared convolutional neural network. $image_i$ represents the image information at the i-th position in the network. h_{IMA}^{i} represents the feature information of the image. Afterwards, the image scene information is fused and processed. Finally, all image data information is connected through the connection layer of the convolutional neural network, as shown in Eq. (5).

$$h_{CSI} = FC\_layer(\bar{h}_{IMA}) \tag{5}$$

In Eq. (5), h_{CSI} represents the size of the feature extraction vector for the visual image. $FC\_layer(\bar{h}_{IMA})$ represents the feature vector of the connection layer.

B. Fingerprint Device Image Recognition and Positioning Method

Visual image extraction and data sharing can achieve feature extraction of visual images in space, but there are still positioning deviations and unstable data collection in the model. The second problem of fingerprint collection and recognition in reconnaissance still needs to be solved. CTGN can collect data from different image information and perform localization, recognition, and analysis on fingerprint images in changing indoor environments. CTGN can convert image information of different styles without data matching and preserve the data information of the images. Fig. 4 displays its network structure.

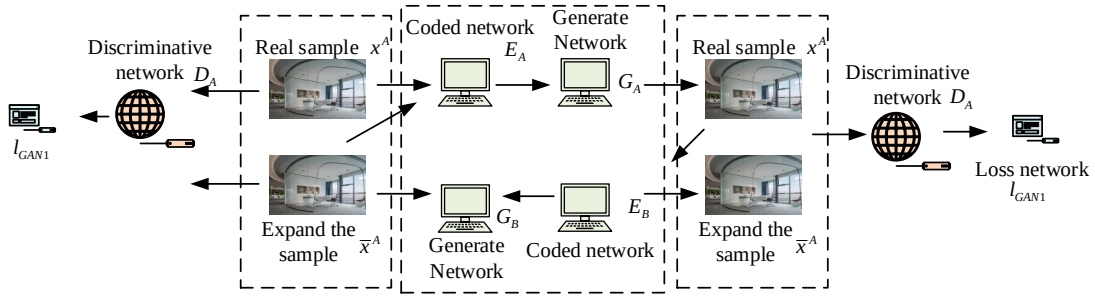

Fig. 4. Cross temporal generative network structure.

From Fig. 4, the network structure includes a judgment structure for image data. The information in the judgment structure is obtained through the loss of positional information in the encoding network and the generative network. Among them, network information will be obtained for sample judgment, which is divided into real samples and expanded samples. The dataset under indoor spatial conditions is divided into A and B. The upper layer network structure is a mapping from A to B, and the output data sample is x_a. The output data sample from the mapping from B to A is x_b. Encoding network and generative network are added to the structure. The encoding network encodes the positional information of samples. The generative network generates corresponding expanded data samples. The judgment network judges whether the input data sample is a real sample or an expanded sample. The loss function in the network model consists of two parts: adversarial loss function and localization information loss function. Eq. (6) displays the network structure adversarial loss function [17].

In Eq. (6), G_A represents the sample of A in the generative network. G_B represents the sample of B in the generative network. D_A represents the judgment network of A. D_B represents the judgment network of B. $E_{x^A \in S_R^A}$ represents the training set of dataset A. $E_{x^B \in S_R^B}$ represents the training set of the dataset B. $l_1(G_A, D_B, A, B)$ represents a set of loss functions. $D_b(x^b)$ represents the judgment network parameters of the real sample A. $D_B((G_A(E_A(x^A))))$ represents the judgment network parameters of the real sample B. Some similar sample sets are existed in the expanded samples. Therefore, the adversarial loss function of the judgment network is shown in Eq. (7).

$$l_1(G_A, D_B, A, B) = E_{x^B \in S_R^B}[\log D_B(x^B)] + E_{x^A \in S_R^A}[\log(1 - D_B((G_A(E_A(x^A)))))] \quad (6)$$

$$l_2(G_B, D_A, B, A) = E_{x^A \in S_R^A}[\log D_A(x^A)] + E_{x^B \in S_R^B}[\log(1 - D_A((G_B(E_B(x^B)))))] \quad (7)$$

At this point, the data objectives that need to be optimized in the network model are shown in Eq. (8).

$$\min_{G_B} \max_{D_A} l_2(G_B, D_A, B, A) \quad (8)$$

Calculating the adversarial loss function can perform image style analysis between two spatiotemporal regions. However, for the positioning of fingerprint devices, it is necessary to expand the data and constrain the data information. For the real sample data in space, it can be mapped into the same position space. Eq. (9) displays the current generated mapping feature vector size.

$$E_B(\bar{x}^B) = E_B(G_A(E_A(x^A))) \approx E_A(x^A) \quad (9)$$

In Eq. (9), $\bar{x}^B$ represents the expanded sample data. Similarly, for sample data A, the above formula conditions are also applicable. The main purpose of network structure is to map the maximum and minimum data of the network parameters generated by the entire data, as shown in Eq. (10) [18].

$$G_A^*, G_A^* = \arg \min_{G_A, G_B} \max_{D_A, G_B} l_{CSGN}(G_B, G_A, D_A, D_B) \quad (10)$$

In Eq. (10), G_A^*, G_A^* represents the mapping effect of network parameters generated through data. The judgment network generates parameters and fixes the generative network parameters. Then, the generative network parameters are replaced and recalculated, which achieves the maximum and minimum judgment of the model mapping relationship. When locating spatial positions, it is necessary to locate and judge a fingerprint signal at a specific time and state. Eq. (11) represents the size of the fingerprint signal dataset.

$$D_m = \{(x_i^m, y_i^m)\}_{i=1}^{Nm} \sim p^m(X, Y) \quad (11)$$

In Eq. (11), D_m represents the dataset in the spatiotemporal domain. X represents sample spatiotemporal. Y represents the spatiotemporal position of the sample. x_i^m represents the i-th signal sample in spatial region m. y_i^m represents the G-th signal sample in the spatial position region m. $p^m(X, Y)$ represents the data distribution in the m-th spatial and spatial location area. A new network model structure is obtained by analyzing the spatial location of the network model and fingerprint, as shown in Fig. 5.

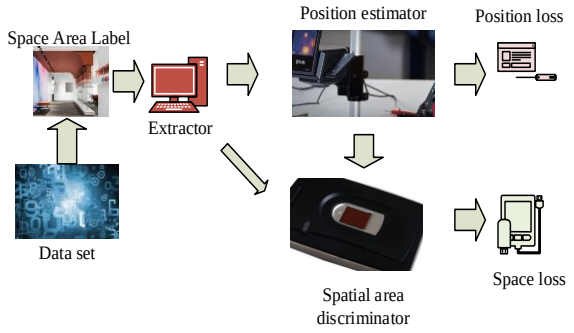

Fig. 5. Structure of fingerprint spatial network model for localization analysis.

From Fig. 5, during the training of network data, image data, coordinate data, label data, and CSI data are extracted from the data. Then, the fingerprint signal is extracted using a fingerprint data extractor to obtain the fused fingerprint signal. The spatial position calculation formula mentioned above is used to calculate the fingerprint position. The feature data of the fingerprint also needs to be identified and analyzed through a discriminator. The adversarial loss function and spatial position loss function are obtained. Finally, the integration of fingerprint data and network structure is completed. The fingerprint adversarial loss function in the network is shown in Eq. (12).

$$l_y(\theta_f,\theta_y)=-\sum_{m=1}^{M}\frac{1}{N_m}[\sum_{i=1}^{Nm}\sum_{j=1}^{N_{RPs}} y_i^m(i)\log(\hat{y}_i^m(j))] \quad (12)$$

In Eq. (12), y_i^m represents the position data obtained from the training samples in the data. N_{RPs} represents the number of reference points for fingerprints, which is the total number of fingerprint positions. θ_f represents a spatial discriminator. θ_y represents a position discriminator. $l_y(\theta_f,\theta_y)$ represents the adversarial loss function value. $\hat{y}_i^m$ represents the probability distribution of the data estimator position. The spatial position loss function of the network is shown in Eq. (13) [19].

$$l_d(\theta_f,\theta_d)=-\sum_{m=1}^{M}\frac{1}{N_m}[\sum_{i=1}^{Nm}\sum_{j=1}^{N_{RPs}} d_i^m(i)\log(\hat{d}_i^m(j))] \quad (13)$$

In Eq. (13), $l_d(\theta_f,\theta_d)$ represents the loss function of spatial position. θ_d represents a region discriminator. d_i^m represents the spatial data information obtained from training samples in the data. d_i^m represents the probability distribution of the region discriminator location. Finally, to achieve precise positioning of fingerprint devices and image recognition in indoor spaces, a new fingerprint positioning framework model is built on the basis of the network model, as shown in Fig. 6.

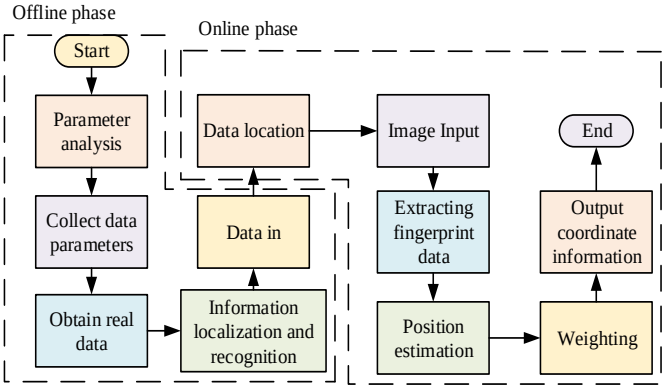

Fig. 6. Fingerprint localization framework model.

From Fig. 6, the framework is mainly divided into two stages: offline and online. Offline state analyses data parameters for coordinate images and CSI of reference point positions in space. Simultaneously collecting data parameter information from these aspects can yield more authentic and effective data. Afterwards, unknown information is located and identified through the above network structure. The obtained data information is transmitted to the network structure. It is input into the online stage through the network structure. In the online stage, real-time image input is completed by locating the data. The spatial fingerprint extractor is used to extract the fingerprint data. Then the fingerprint position is estimated and analyzed through the position estimator. The network model is weighted and processed. Finally, the coordinate information of the position is output.

IV. Analysis of Fingerprint Device and Artificial Intelligence Image Fusion Method

This section mainly analyzes the effectiveness of the current model parameters used to explore their practical application effects under different parameters. Secondly, the recognition and fingerprint localization performance of the model are compared with traditional methods through experiments.

A. Model Performance Parameter Testing and Analysis

To study the performance of the model, the multi-directional signal data of the image data is collected. The wireless network device used is Intel5300. The network data received signal size is 20MHz. The wireless network signal received is placed in the corner for signal data collection in four directions. The experiment uses different spaces for fingerprint recognition research. The collected data includes indoor and outdoor environments. To test the training effect of the current model on different spatial domains, fingerprint localization errors are compared in different spatial domains. The spatial domain sizes calculated in the previous section are denoted as CSI_1 and CSI_1, CSI_2. CSI_1, CSI_2, CSI_3 and $CSI_1, CSI_2, CSI_3, CSI_4$ are used as spatial domain size comparison parameters, as shown in Fig. 7.

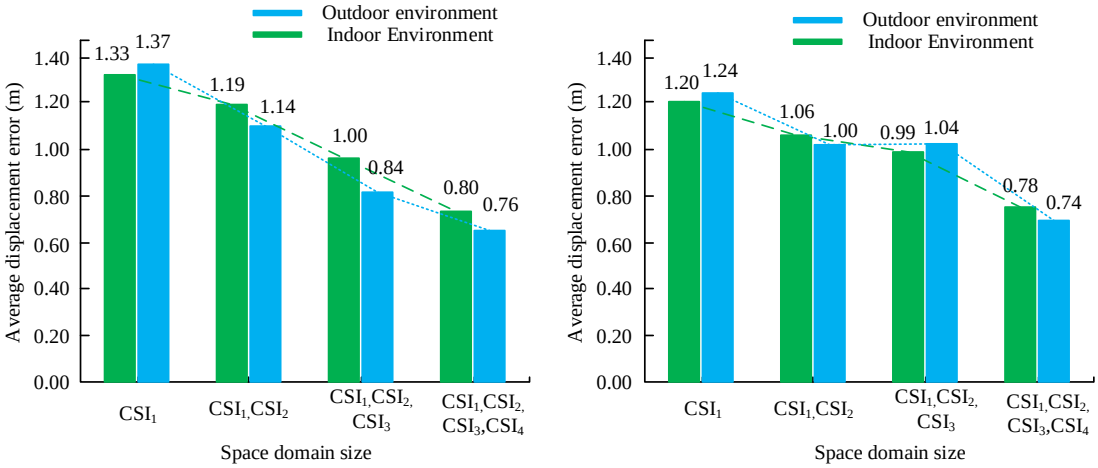

(a) Comparison of different spatial domains in Data 1 (b) Comparison of different spatial domains in Data 2

Fig. 7. Comparison of positioning errors in different spatial domain sizes.

From Fig. 7 (a), the average positioning error of the model varied in different space domains. In the $CSI_1, CSI_2, CSI_3, CSI_4$ space domain, its average positioning error value was the smallest. Compared with the highest error value, its outdoor average error was 0.53m smaller and the indoor average error was 0.61m smaller. In Fig. 7 (b), the minimum average positioning error still appeared in the $CSI_1, CSI_2, CSI_3, CSI_4$ space domain. The minimum error values for outdoor and indoor environments were 0.78m and 0.74m, respectively. Compared with CSI_1 with the highest average error value, its error value distribution was 0.42m and 0.50m lower. When the space domain was $CSI_1, CSI_2, CSI_3, CSI_4$, the model had the best positioning effect and the lowest positioning error. The commonly used image fusion methods, including Stage Data Fusion (SDF), Threshold Data Fusion (TDF), and Tensor Fusion (TF), are compared to obtain the required parameter data for localization, as shown in Table I. A smaller cosine distance indicates better performance of the model.

From Table I, in the indoor cosine distance comparison of the model, the shortest cosine distance of the proposed model was only 0.076. Compared with the highest SDF model, it was 0.208 lower. The proposed model used in outdoor environments was 0.206 lower than the highest model. In the comparison of the average running time, the running time of the proposed model was shorter, indicating that the running speed and efficiency of the model used in the study were faster and higher. The model had better model performance compared with traditional models.

B. Analysis of Fingerprint Localization Effect

Comparative tests are conducted on different data localization methods, such as Received Signal Strength Indicator (SSI), Time Difference of Arrival (TDOA), and Angle of Arrival (AOA), to obtain the positioning error. Fig. 8 displays the results.

TABLE I. COMPARISON OF MODEL FINGERPRINT LOCALIZATION PARAMETERS

Environment	Cosine distance of fingerprint features in different spatial domains	Average cosine distance	Training frequency	Average positioning time (s)
Indoor Environment	SDF	0.284	100	0.054
	TDF	0.265	100	0.056
	TF	0.245	100	0.064
	CTGN	0.156	100	0.026
	Research model	0.076	100	0.012
Outdoor environment	SDF	0.282	100	0.058
	TDF	0.263	100	0.064
	TF	0.241	100	0.034
	CTGN	0.157	100	0.022
	Research model	0.076	100	0.013

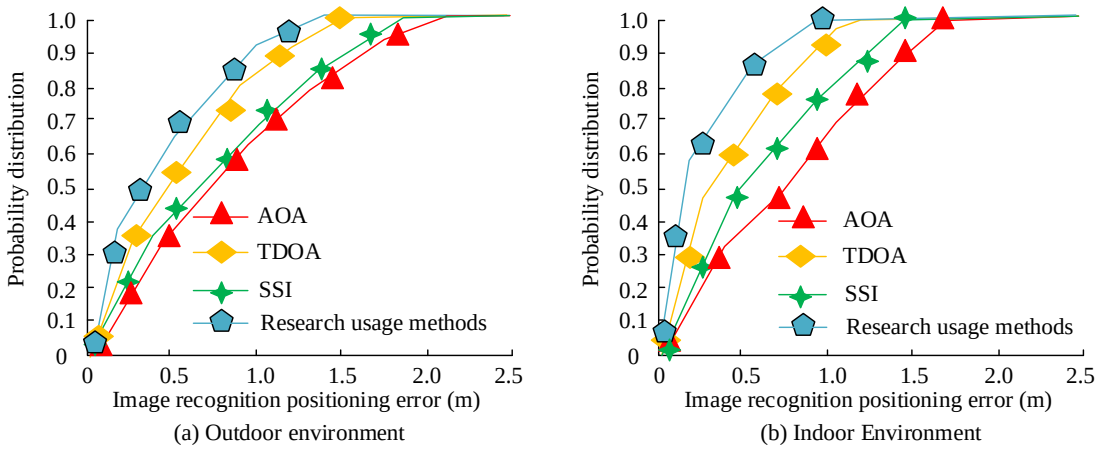

Fig. 8. Comparison of positioning errors of different models.

From Fig. 8 (a), in the outdoor environment, the error values of the four models increased with the increase of the positioning point probability distribution, and then tended to stabilize. When the probability distribution is 100%, the positioning error value of the positioning model reached its maximum. The maximum positioning error value of the research model was 1.3m, while the maximum positioning error values of the AOA, TDOA, and SSI were 2.0m, 1.5m, and 1.7m, respectively. The positioning error value of the model used in the study was smaller, which was 0.7m, 0.2m, and 0.4m lower than the three models, respectively. From Fig. 8 (b), in indoor environments, the minimum positioning error value of the model used in the study was 0.9m. Compared with the 1.0m, 1.4m, and 1.6m of the other three models, the model used in the study had a lower positioning error value. The model used in the study performed better in data image localization. From the figure, the indoor positioning error value was smaller, which may be due to the smaller indoor environment space and fewer measured position points. The fusion network used in the study is a CTGN. Therefore, to test the effectiveness of the current fusion network in image position information localization, different fusion methods are compared. The test results are shown in Fig. 9.

From Fig. 9 (a), in indoor environments, the positioning error value based on the spatiotemporal fusion method was even smaller, only 1.6m. The positioning error values of SDF, TDF, and TF for other fusion methods were 4.1m, 3.4m, and 2.4m, respectively. Compared with the spatiotemporal fusion method, other methods had larger positioning error values, which were 2.5m, 1.8m, and 0.8m higher than the methods used in the study, respectively. The spatiotemporal fusion method used in the study showed better performance in locating indoor environments. From Fig. 9 (b), in the outdoor environment, the fusion method used in the study has a positioning error of 2.1m, which is also significantly smaller than other fusion methods. However, from the comparison of indoor and outdoor environments in the above figure, the positioning error value of the outdoor environment should be greater than that of the indoor environment. From the figure, except for the method used in the study, the positioning error values of the other three fusion methods were relatively small, but the difference was not significant. This may be due to the low requirements of other fusion methods for spatial position positioning, resulting in little difference in the error data values between indoor and outdoor. To test the fingerprint recognition accuracy of the research model, it is compared with the other fusion methods mentioned above. The results are shown in Fig. 10.

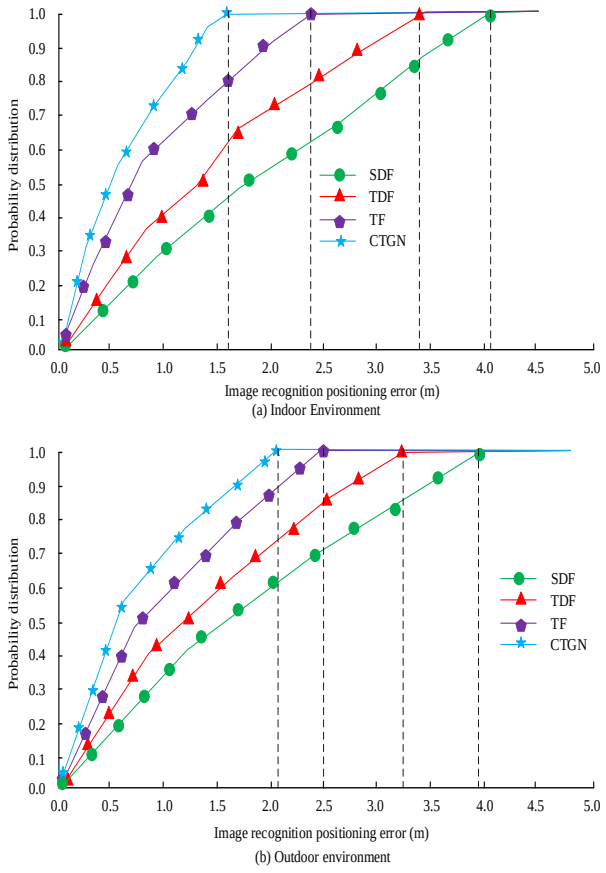

Fig. 9. Comparison of positioning errors between different fusion methods.

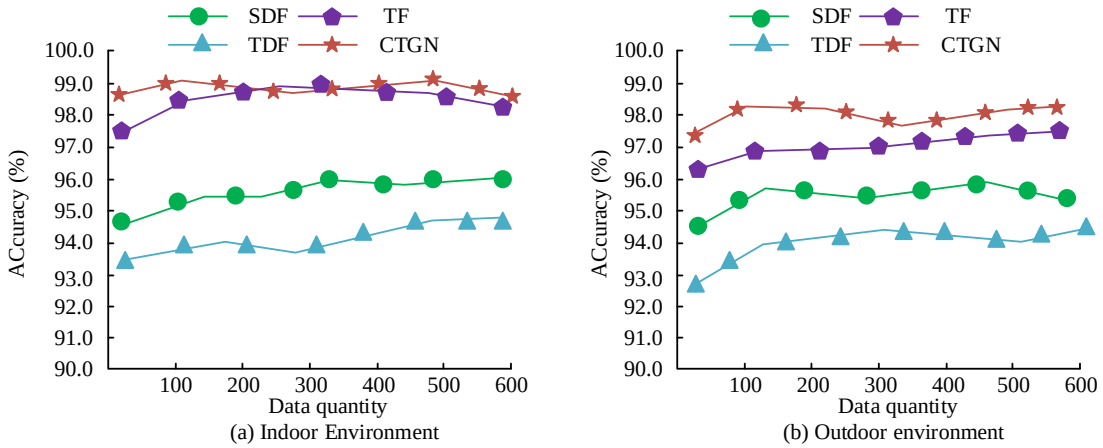

Fig. 10. Comparison of accuracy of different fusion methods.

From Fig. 10 (a), the fingerprint recognition accuracy of the four methods increased with the increase of data, and then tended to a relatively stable state. However, the overall curve changes showed fluctuations. This may be due to the fact that when fingerprint data is used for localization and recognition, the accuracy of the model is lower due to the larger dataset. However, the accuracy of the research method was higher, with an average accuracy of about 98.6%, which was about 4.5% higher than the TDF fusion method with the lowest accuracy of 94.1%. From Fig. 9 (b), the accuracy of the research method was higher than other methods, with an average accuracy of about 97.8%, which was about 3.6% higher than TDF model with the lowest accuracy of 94.2%. The research method had a higher accuracy in fingerprint recognition. To test the application effectiveness of the current research model in several traditional models, the recall rate, F1 value, and recognition error in fingerprint recognition positioning data are compared. The analysis results are shown in Table II.

TABLE II. PERFORMANCE COMPARISON OF DIFFERENT MODELS

Model	Recall (%)	F1	Average percentage error	Root mean square error
SDF	88.62	0.53	6.53	6.58
TDF	89.65	0.68	7.65	6.35
TF	90.15	0.96	5.32	5.78
CTGN	92.35	0.75	5.96	5.48
SSI	88.68	0.64	4.36	5.62
TDOA	91.25	0.88	5.87	4.35
AOA	90.64	0.92	3.56	4.36
Research model	96.35	0.99	2.35	2.15

In Table II, in terms of recall rate, the highest recall rate of the research method was 96.35%. The average percentage error value was the smallest among several models, with a median of 2.35. Compared with the TDF with the highest recall rate, it was 5.30 lower. The root mean square error value of the research method was also the smallest, at 2.15, which was 4.43 lower than the SDF model with the highest recall rate. From this, the research method showed good model performance in fingerprint recognition and localization.

V. CONCLUSION

A fusion algorithm model combining artificial intelligence and spatiotemporal domain algorithms is proposed to address the insufficient accuracy in fingerprint image extraction and localization in different investigation environments, as well as difficulties in collecting fingerprint localization data. The research results indicated that the optimal space domain size for the model was $CSI_1, CSI_2, CSI_3, CSI_4$. The minimum error values for outdoor and indoor environments were 0.78m and 0.74m, respectively. The cosine distance of the research model was the shortest, only at 0.076. Compared with the highest SDF model, it was 0.208 lower. The maximum positioning error value of the model used in the study was 1.3m, which was 0.7m, 0.2m, and 0.4m lower than other models, respectively. The minimum positioning error value for the proposed model in indoor environments was 0.9m. Compared with other models at 1.0m, 1.4m, and 1.6m, the positioning error value of the research model was lower. Compared with the spatiotemporal fusion method, other methods had larger positioning error values, which were 2.5m, 1.8m, and 0.8m higher than the methods used in the study. The accuracy of the research method was higher, with an average accuracy of about 98.6%, which was about 4.5% higher than the TDF fusion method with the lowest accuracy. The root mean square error value of the research method was also the lowest, only at 2.15, which was 4.43 lower than the highest SDF model. The performance of the research model is significantly better than traditional methods. It has better results in data processing. Although some achievements have been made in the research, there are still some problems, such as the small amount of data used in the study. Therefore, more and larger data will be used for analysis and research in the future.

REFERENCES

[1] Chen C Y, Lai I C, Wu P Y, Ruey-Beei Wu.Optimization and Evaluation of Multidetector Deep Neural Network for High-Accuracy Wi-Fi Fingerprint Positioning. IEEE internet of things journal, 2022, 16(9):15204-15214.

[2] Shang J, Yao Z.Study in CSI Correction Localization Algorithm with

DenseNet. IEICE Transactions on communications, 2022, 105(1)76-84.

[3] Yan J, Ma C, Kang B, Xiaohuan Wu. Extreme Learning Machine and AdaBoost Based Localization Using CSI and RSSI. IEEE Communications Letters, 2021, 25(6):1906-1910.

[4] Pu Q, Ng K Y, Zhou M, Wang, Jie.A Joint Rogue Access Point Localization and Outlier Detection Scheme Leveraging Sparse Recovery Technique. IEEE Transactions on Vehicular Technology, 2021, 70(2):1866-1877.

[5] Zhu X, Qiu T, Qu W, Xiaobo Zhou, Mohammed Atiquzzaman. BLS-Location: A Wireless Fingerprint Localization Algorithm Based on Broad Learning. IEEE Transactions on Mobile Computing, 2021, 22(1):115-128.

[6] Labinghisa B A, Lee D M. Neural network-based indoor localization system with enhanced virtual access points.Journal of supercomputing, 2021, 77(1):638-651.

[7] Zhang Y, Psounis K. Efficient Indoor Localization via Switched-Beam Antennas. IEEE Transactions on Mobile Computing, 2020, 19(9):2101-2115.

[8] Li L, Guo X, Zhao M,Huiyong Li. TransLoc: A Heterogeneous Knowledge Transfer Framework for Fingerprint-Based Indoor Localization. IEEE Transactions on Wireless Communications, 2021, 20(6):3628-3642.

[9] Zhou C, Liu J, Sheng M, Zheng Yang, Li Jiandong. Exploiting Fingerprint Correlation for Fingerprint-Based Indoor Localization: A Deep Learning Based Approach. IEEE Transactions on Vehicular Technology, 2021, 70(6):5762-5774.

[10] Li Q, Liao X, Liu M, Shahrokh Valaee. Indoor Localization Based on CSI Fingerprint by Siamese Convolution Neural Network. IEEE Transactions on Vehicular Technology, 2021, 70(11):12168-12173.

[11] Tan J, Wu H, Chow K H, S.-H. Gary Chan. Implicit Multimodal Crowdsourcing for Joint RF and Geomagnetic Fingerprinting. IEEE Transactions on Mobile Computing, 2021, 22(2):935-950.

[12] Li S, Fu M, Zhu X. An Indoor Localization Algorithm Based on Markov State Iterative Analysis and Fingerprint Clustering Structural Optimization. IET Communications, 2020, 14(11),1687-1695.

[13] Xue W, Yu K, Li Q, Baoding Zhou. Eight-Diagram Based Access Point Selection Algorithm for Indoor Localization. IEEE Transactions on Vehicular Technology, 2020, 69(11):13196-13205.

[14] Ghosh M, Singh A, Borah S S, John Vista. MOSFET-Based Memristor for High-Frequency Signal Processing. IEEE Transactions on Electron Devices, 2022, 69(5):2248-2255.

[15] Hasan M M, Nasrabadi N, Dawson J. On improving interoperability for cross-domain multi-finger fingerprint matching using coupled adversarial learning. IET Biometrics, 2023, 12(4):194-210.

[16] Chengqi M A, Wu B, Poslad S, David R. Selviah. Wi-Fi RTT Ranging Performance Characterization and Positioning System Design. IEEE Transactions on Mobile Computing, 2022， 21(2):740-756.

[17] Tianren Z, Ning W, Riggleman R A. Failure and Mechanical Properties of Glassy Diblock Copolymer Thin Films. Macromolecules, 2022, 55(24):10880-10890.

[18] Tao Y, Zhao L. Fingerprint Localization with Adaptive Area Search. IEEE Communications Letters, 2020, 24(7):1446-1450.

[19] Pal S, Roy A, Shivakumara P, Pal U. Adapting a Swin Transformer for License Plate Number and Text Detection in Drone Images. Artificial Intelligence and Applications, 2023, 1(3), 145-154.